AGN Beyond the 100pc Scale

R A E Fosbury

Space Telescope - European Coordinating Facility, Garching bei München, Germany; rfosbury@eso.org

1 Introduction

Galaxies and their nuclear SuperMassive Black Holes (SMBH) appear to be intimately related components of the same fundamental formation and evolutionary process [3], [7]. When the host galaxy contrives to feed its nuclear monster, it unleashes a torrential energy output that can far outshine the gentler and, apart from the occasional supernova, more constant shining of the stellar populations. The observed proportionality between the masses of the black hole and the galaxy bulge (see chapter 8 of this volume) suggests a close coupling—a negative feedback loop—that limits SMBH growth. One of our more important goals is to understand the nature of this mechanism. To do this, we must look at the galaxy and its larger environment, not at the nuclear regions alone.

A brightly shining AGN does us a useful service by illuminating its host galaxy with an ionizing radiation field. The 'fluorescent emission' that this produces can be studied to tell us about some rather fundamental galaxy properties such as, via emission line kinematics, the mass and, via line ratios and ionization modelling, the chemical composition of the interstellar medium (ISM). This is particularly pertinent to the studies of galaxies at early epochs (high redshift) where the hosts are exceedingly faint in the absence of such excitation. Such investigations are crucial for our picture of the assembly of massive galaxies and the chemical enrichment that is an integral part of the process.

With a luminosity that can far exceed that of its host, an AGN will not only illuminate its surroundings, it will push material around. Radiation pressure will affect dust clouds, ambient gas will be shocked in the presence of the particle jets, flows will be driven and the ISM will be generally mixed and redistributed. All these processes have to be recognised and understood if we are to generate a complete picture.

We know that an active galaxy possesses an intrinsic axial symmetry due to the spin of the SMBH. This symmetry leaves its imprint on the host in the form of an anisotropic illuminating radiation field and the effects of the jets that initially trace the AGN spin axis. This has the important consequence that active galaxies appear quite different when viewed from large and small angles to the AGN spin axis. The unravelling of these orientation effects, and

the realisation that the purely empirical AGN classification schemes had to be recrafted, was the work of the last two or three decades. The orientation-based unification of AGN (type 1 viewed $\sim$ pole-on; type 2 $\sim$ equator-on) is now well-established [5] and we have moved on to the next, and intrinsically more interesting, task of delineating the more subtle evolutionary processes.

Finally, and this is perhaps the most fundamental question of all, we want to see the role of the AGN in the energy balance of the Universe as a whole. What fraction of the overall photon energy production comes from gravity (matter collapse onto SMBH) and what fraction from nucleosynthesis (element transmutation in stars) and how does this ratio change with cosmic epoch [19]? The observations tell us that the ratio has been not so enormously different from unity. Is this another cosmic coincidence or is it an inevitable consequence of the laws of nature? To answer this question, we need to find all the AGN in the Universe and then to measure their bolometric luminosities. The host galaxies can serve as the 'bolometers' that measure the output of the type 2 objects whose AGN we do not see directly.

The aim of this chapter is not to give an exhaustive review of 'extranuclear' activity. Rather, by choosing some illustrative examples, we can construct a catalogue of the more important AGN–host galaxy interactions and so equip ourselves to attack the unsolved fundamental questions concerning the relationship between the compact structures at the nucleus and their large-scale galactic surroundings.

2 AGN–host Interactions

The host galaxy 'feels' the presence of its nuclear SMBH through the gravitational effect of its mass, through the ionizing and non-ionizing radiation field emitted by the AGN and by the particle flows in the jets and radiation pressure driven winds with any associated magnetic fields. In this chapter, our concern lies principally with the radiation field and with the AGN-related flows.

2.1 The AGN Radiation Field

The primary radiation source associated with the SMBH is assumed to be more-or-less isotropic. However, beyond the scale of 100pc, this intrinsic isotropy may have been destroyed by absorption, most notably by the presence of an optically thick equatorial torus surrounding the black hole (see chapter 4). Such a structure can produce sharply defined shadows and it is thought to be responsible for most, if not all, of the 'ionization cones' first seen in the emission line images of Seyfert galaxies [13]. A schematic illustration of the origin of this form of isotropy is shown in Fig. 1.

As their name implies, the ionization cones are delineated by the shadowing of the AGN radiation below the Lyman limit at 912Å. The optical

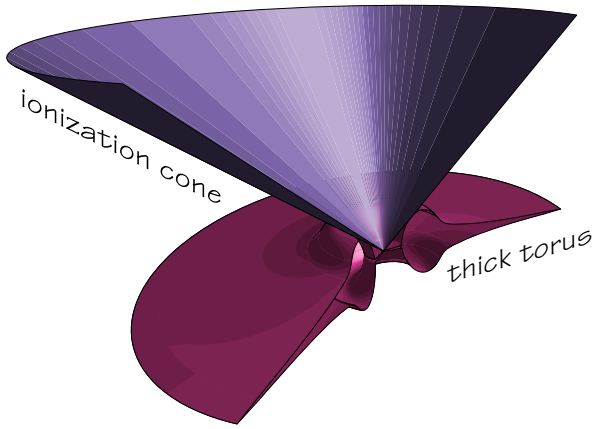

Fig. 1. A sketch of the optically thick nuclear torus whose shadow produces a sharply defined 'ionization cone' of the type that is commonly seen in Seyfert 2 galaxies.

properties of the torus will clearly vary with wavelength and it is expected to become transparent, in some objects, in the hard X-ray band and also somewhere in the mid-far infrared. In an attempt to illustrate how the apparent isotropy varies with wavelength, Fig. 2 gives a schematic view in four wavebands from hard X-rays to the mid-infrared (MIR). Such a concept is useful when designing strategies for finding type 2 AGN in multiband surveys.

The radiation field affects the material within these ionization cones in a number of ways, each of which produces characteristic observable phenomena. The photoionization process results in a spatially extended emission line region which is variously known as the Extended Emission Line Region (EELR) or the (Extended) Narrow Line Region (ENLR). The term 'narrow' is used to contrast this region with the much smaller—and much less massive—Broad Line Region (BLR) surrounding the nucleus. The emission line widths actually extend over a broad range of values from the relatively quiescent interstellar medium of the galaxy which happens to be illuminated by the nucleus, to material that may be shocked by AGN-driven winds or jets. In many objects, there appears to be a correlation between line width and ionization state that may reflect either differences in density or the presence of alternative ionization mechanisms [10]. A notable characteristic of the NLR is the wide range of ionization levels present in the gas. This is a product of the shape of the ionizing Spectral Energy Distribution (SED) emitted by the AGN which extends from the Lyman limit up to very high energies and is markedly different in its effects from a black body-like stellar ionizing spectrum. The high energy photons can penetrate deep into clouds that are optically thick to the Lyman continuum where they partially ionize

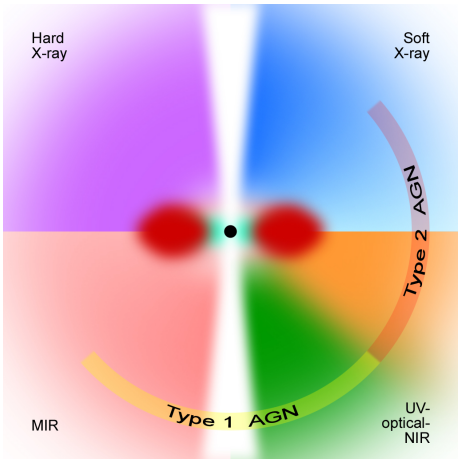

Fig. 2. A schematic representation of the apparent anisotropy of the AGN radiation field in different wavebands. The torus is essentially opaque from the MIR through to the soft X-ray but can become transparent outside this range. This pattern is useful for identifying type 2 AGN in multiband surveys. The spin axis has been left clear to indicate the possible presence of a particle jet and its associated, beamed radiation field.

and heat a predominantly neutral gas, resulting in the coexistence of lines from [O I], [N I], [S II] etc. with lines from much more highly ionized species including, sometimes, even the 'Coronal' lines such as [Fe X] [9].

The presence of dust within the ionization cones has a number of consequences. AGN photons can ionize dust grains, donating high kinetic energy electrons to the gas and so affecting the thermal balance. The photons can also efficiently transfer momentum to grains and thus, by dragging the gas along with them, produce radiation pressure driven winds. The presence of these winds can be inferred from the emission line shifts and widths. Another consequence of dust is the result of its high cross section for scattering. Dust clouds can act as 'mirrors' that allow us to see the AGN along indirect sightlines in sources where the AGN is obscured. The presence of scattered light can be most directly inferred by measuring linear polarization. In the axisymmetric bi-conical geometry of an AGN, a net linear polarization—with the $\boldsymbol{E}$-vector perpendicular to the cone axis—can remain even after the spatial averaging by the polarimeter of unresolved sources. Hot electrons can also Thompson-scatter and, hence, polarize, AGN radiation although electrons are far less efficient scatters than dust grains, and clouds with sufficient Thompson optical depth appear quite rare away from the immediate nuclear environment. Electron-scattered spectra will be significantly smeared in wavelength due to high Doppler velocities in a hot, highly ionized plasma. The presence of broad-line (type 1) AGN is, indeed, demonstrated in polarized light in many type 2 objects. The energy absorbed—rather than scattered—

by the dust will be re-radiated somewhere in the mid-far infrared (MIR, FIR), depending on the equilibrium temperature attained by the dust grains in a given AGN radiation field and at a given radial distance [15]. In general, such AGN-heated dust will compete with starburst-heated dust to dominate the FIR emission from an active galaxy.

2.2 Winds and Jets

The process of accretion onto the SMBH results in the generation of substantial amounts of kinetic energy. This is transported both in the form of highly collimated jets (see chapter 2), seen predominantly in radio-loud sources, and as more isotropic winds. The evidence from some (radio quiet) Broad Absorption Line (BAL) QSOs suggests that fast winds can carry a substantial fraction of the AGN power, perhaps even approaching that of its radiative output. While the AGN radiation field produces its dominant effects on the ISM of the host galaxy, the winds and jets probably transport their energy to larger scales and dissipate it in the tenuous—and already hot—intergalactic medium (IGM). The passage of this kinetic energy through the galaxy can, however, influence the way the ISM is distributed and, by driving shocks, increase the gas density in some regions. Both the shocks themselves, and the density changes they produce, can influence the line emission from the gas in the galaxy.

Powerful radio galaxies such as *Cygnus A* possess energetic jets that inflate huge cocoons which are overpressured with respect to the surrounding IGM and expand supersonically into it. More generally, however, the jet-inflated cocoons behave as buoyant bubbles and dissipate energy rather gently. Whilst most of the power in the jets is in the form of bulk kinetic energy, the inner regions, which are moving relativistically in some powerful radio sources, can produce a Doppler boosted photon 'beam' with a rather small opening angle. For observers within the radiation pattern of such a beam, the source will appear as a *blazar* or a *BL Lac* object. The SED of such a beam will differ from that of the more isotropic AGN radiation field and, although it may carry only a small fraction of the bolometric luminosity of the AGN, does illuminate regions along the radio axis with a high photon density. If the beams illuminate gas clouds, the ionizing and other effects on them can be substantial. The high photon densities can be maintained in the beam to very large radial distances and so can, in principle, be responsible for ionizing gas even well beyond the extent of the radio lobes.

The reaction of an AGN, in the form of its radiative and kinetic output, to the rate and form of accretion onto the SMBH constitutes a potential 'feedback loop' that can limit growth and, perhaps, establish the apparent observed relationship between the black hole mass and that of the host galaxy bulge (see chapter 8).

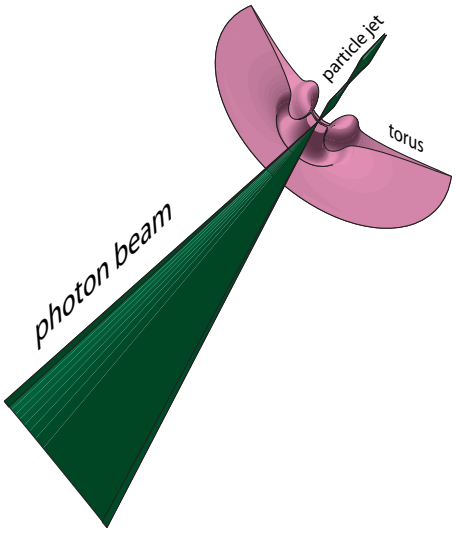

Fig. 3. A sketch showing the relation of the particle jet and associated photon beam to the nuclear torus in a radio-loud AGN. The jet and the beam are both, of course, bi-directional and have only been separated in the diagram for clarity.

3 Observational Techniques and Examples

Most observational work on the AGN – host galaxy connection has been carried out on the type 2 sources—Seyfert 2 rather than Seyfert 1 and radio galaxies rather than quasars—for the simple reason that a direct view of the AGN in type 1 objects results in an excessive 'glare' that renders it difficult to see faint extra-nuclear structures. The presence of thick obscuration close to the nucleus and in our line-of-sight in type 2 sources results in a very effective 'natural coronograph'.

The first indications of the spatial scale of the interaction between an AGN and its host galaxy was the discovery of the EELR which, especially in the radio-loud sources, could extend tens, sometimes hundreds, of kiloparsecs from the nucleus. This realisation came as a result of instrumental developments in the early 1970's. While there had been some work with photographic long-slit spectrographs, the introduction of panoramic electronic detectors such as the Image Photon Counting System (IPCS) and, later, CCDs, made it possible to do quantitative, spatially resolved studies of emission lines in the optical spectrum. Before that, most AGN spectroscopy had been carried out with 1-dimensional spectral scanners that gave little—though not zero—information about the extent of the emission line regions. The general picture that emerged was that the ISM of the host galaxy was being photoionized

by the hard AGN radiation field [12]. The careful correlation of high resolution radio continuum maps made with interferometric arrays, notably in Cambridge, Westerbork and the Very Large Array (VLA) in New Mexico, suggested, however, that the jets were influencing the distribution and possibly also the excitation of the gas. It was learned that it was not only the radio-loud AGN that had bi-symmetric jets. The much less radio luminous Seyfert galaxies also contained radio nuclei, often with extended structures exhibiting axial symmetry.

Work on the spatial correlations continued with attempts to establish physical connections between the line emitting gas (at $T_e \sim 10^4$K) and the relativistic plasma responsible for the non-thermal radio emission. While there appeared to be an approximate pressure balance between the two components, the interactions were likely to be far from an equilibrium situation. Indeed, later work has shown that the optically emitting gas can have a significantly higher pressure than the surroundings. The effect of shocks, driven by the jets, was not obvious. While shocks are clearly capable of ionizing gas—either collisionally or, in faster cases, radiatively—diagnosing the relative importance of these processes and those produced by the powerful AGN radiation field is complicated and often ambiguous.

Work on the relationship between the radio axis and the symmetry axis (if it has one) of the host galaxy did not produce immediately explicable results. The spiral galaxy hosts of Seyfert galaxies have rotation axes that show no apparent correlation with their AGN axis for the late-type hosts, but a tendency for alignments in the earlier-type hosts. Such work, however, is difficult since jets emerging within the plane of the disc will produce different effects to those emerging close to the pole. The clearest association exists between the cone axis and the elongation of the nuclear radio source—often double or triple—in Seyfert galaxies. In the elliptical galaxy hosts of the radio-loud sources, the situation is less clear since identifying a relevant symmetry axis of a possibly triaxial ellipsoid is both observationally difficult and interpretationally ambiguous. Where a small scale nuclear gas/dust disc can be seen, however, the jet appears to be perpendicular to it.

When observations of radio galaxies at redshifts greater than about 0.6 became routine in the mid 1980's, it was realised that the optical images—corresponding to restframe blue or ultraviolet light—were elongated and shared an axis, although not necessarily a detailed spatial correspondence, with the double-lobed radio source. This became known as the 'alignment effect' and it spawned a great variety of ideas for its physical interpretation [1], [6]. Observations of these sources in the near-infrared (NIR)—corresponding more closely to the restframe optical—showed a weaker effect, indicating that it was the blue/UV light that is aligned. Spatially resolved spectroscopy of these distant objects is very demanding with 4m-class telescopes and it was not possible to decide between explanations based on some reprocessing of AGN power transmitted along the axis or the possibility of star formation

triggered by the interaction between the jet and the ISM. At least for the higher redshift sources, inverse Compton scattering of microwave background photons by the relativistic electrons in the radio jets was a possible contributor. Using 4m telescopes, the presence of a linear polarization signal in some sources with an $\boldsymbol{E}$-vector perpendicular to the radio axis suggested the presence of scattering of light from the AGN but it was not until the availability of the much larger 8–10m telescopes that the details of the scattering process became clear and it was shown that this was the dominant, although not necessarily sole, contributor to the alignment effect in the powerful radio sources [15].

The most recent contribution to the study has come from high spatial resolution X-ray maps of the nucleus, the jets and radio hot-spots and the surrounding cluster environment. Detailed studies of *Cygnus A* with Chandra show what can be achieved (Figs. 4, 5) [17]. The principal components are:

- thermal X-ray emission from the intracluster gas,
- a limb-brightened cavity containing the relativistic gas fed by the jets,
- synchrotron self-Compton emission from the radio hot-spots,
- X-ray emission from the jets themselves,
- soft emission from an extended nuclear source and
- hard emission from an unresolved nuclear source.

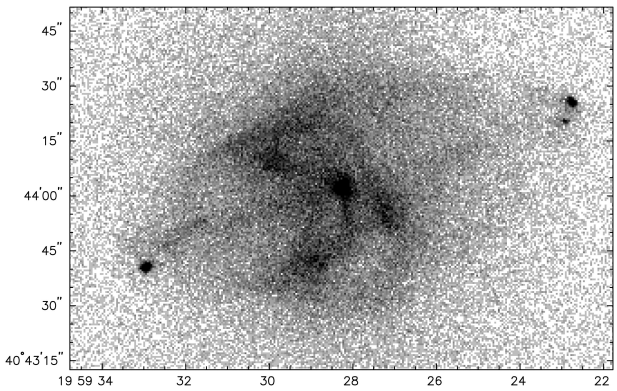

Fig. 4. An X-ray image of *Cygnus A* with the CHANDRA ACIS instrument. (Courtesy A.Wilson et al. NASA/UMD)

The extended nuclear source, on a kiloparsec scale, appears to result from the Thompson scattering of nuclear X-ray photons in a very highly (photo)ionized gas extending along the radio axis. The Thompson optical depth, while it can explain the X-rays, is too small to produce the extended

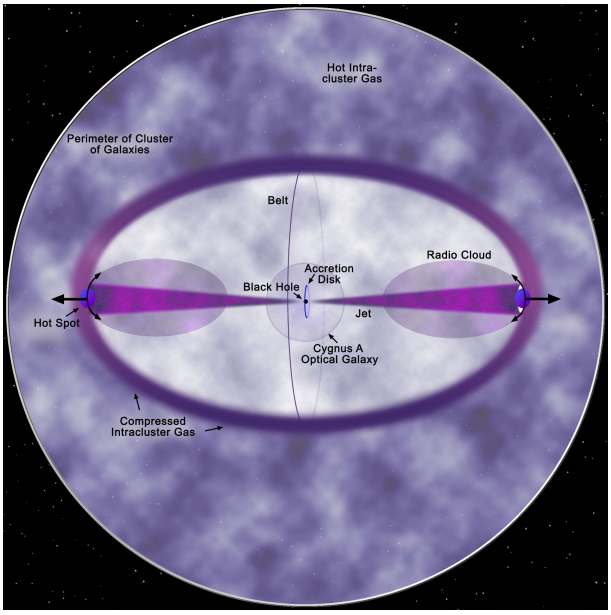

Fig. 5. An X-ray cartoon of *Cygnus A* that illustrates the interactions between the jets and the surrounding intracluster medium. (Courtesy CHANDRA X-ray Observatory, NASA/CXC/SAO)

optical polarization which must, therefore result from dust scattering. The spatial distribution of this soft X-ray component appears to match very closely the emission from the extended coronal lines of [Fe X], [Fe XI], [Ar XI] and [S XII]. This is strong evidence in favour of the photoionization model for the production of the coronal line spectra in AGN in gas with a very high ionization parameter (U = ionizing photon density / particle density).

3.1 Local AGN

Work on the local Seyfert galaxies has concentrated on the nature of the ionization cones (for an example see Fig. 6), their association with the nuclear radio source and their orientation with respect to the host galaxy. Two- and three-dimensional spectroscopy has allowed the study of the ionization state, the kinematic properties and, to some extent, the chemical abundances of the ionized gas. The cones can be seen even in projection against the disc by virtue of their high ionization state and strong line emission (Fig. 7). By taking account of projection effects, either statistically or by direct inference in individual cases, it is possible to infer the true cone opening angle. This, in turn, can be compared with the value implied by the type 1 to type 2 object ratio in samples selected on the basis of an assumed isotropic property.

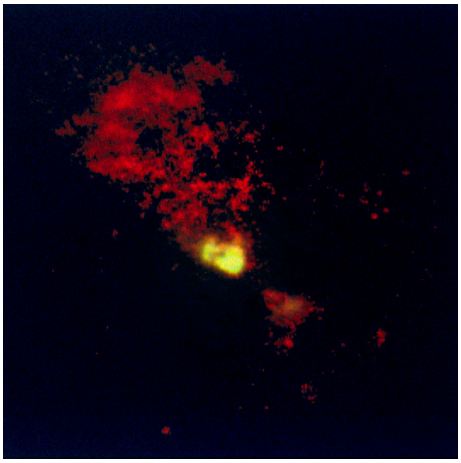

Fig. 6. An early (WFPC) image taken with HST of the ionization cone in the Seyfert galaxy NGC 5728 (Courtesy A.S. Wilson, STScI/NASA). This was taken with the PC before correction of Hubble's spherical aberration. It is in the light of Hα and [O III] and the structure has an overall extent of some 1.8kpc. The apex of each cone indicates, presumably, the site of the obscured AGN.

Fig. 7. An HST WFPC 2 image of the Circinus galaxy in two narrow (Hα and [O III]) and two broad (NIR and green) filters. The nearside ionization cone can be seen projected against the disk by virtue of its strong hydrogen and oxygen line emission. (Courtesy A.S. Wilson et al., NASA)

Cygnus A is also a good relatively low redshift ($z = 0.056$) example of the range of phenomena that can be studied in a powerful radio galaxy. This famous object did, however, strongly resist attempts to fit it comfortably into the emerging orientation-based unification paradigm. There were several

unsuccessful attempts to measure the linear optical polarization that might have been expected in a type 2 object harbouring a powerful quasar. It took the application of the Keck polarimeter and a careful subtraction of the elliptical galaxy starlight to reveal the dust scattering (Fig. 8 - left) [8]. The task was rendered more difficult by the relatively high Galactic extinction in the direction of Cygnus.

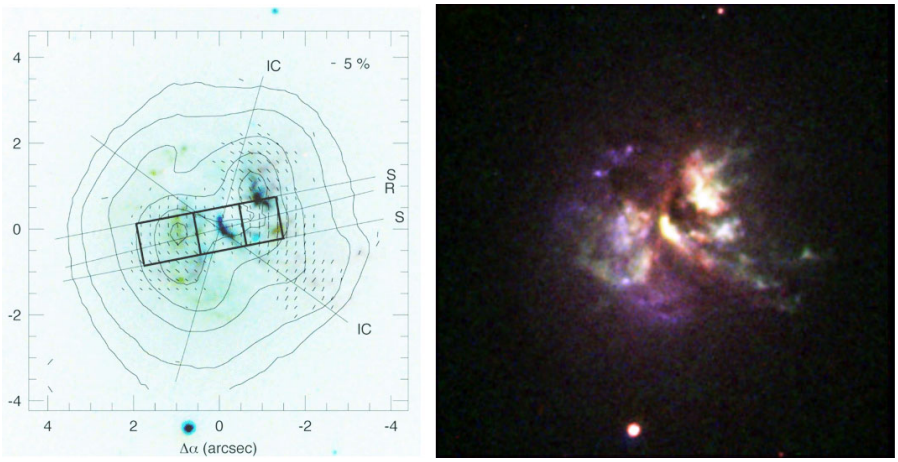

Fig. 8. The powerful radio galaxy *Cygnus A*. The colour image on the right is a combination of B, V, R and I broad band and [O III] and Hα narrow band exposures from the HST WFPC 2 archive with the addition of a B-band exposure with Keck. The B-band contour map on the left is from the Keck LRISp polarimeter showing the measured $\boldsymbol{E}$-vectors and the location of the apertures used for spectropolarimetry (a negative version of the colour image is shown as an underlay). The position of the radio axis (R) and the outline of the ionization cone (IC) are shown. The blue, equatorial ring on the southeast side consists of starlight and is unpolarized.

Images obtained from the ground had never had quite the spatial resolution necessary to make sense of the rather complex optical source structure. It was the assembly of the Hubble images into a colour composite that showed clearly the ionization cones and the ∼4.5kpc diameter ring of blue stars. The combination of large telescope spectropolarimetry and HST imaging allowed, for the first time in this type of object, the direct identification of spatial features with spectral components having a particular polarization pattern and colour (Fig. 9).

The interaction between a powerful radio jet and a substantial obstacle, such as a dwarf satellite galaxy, is a rather rare phenomenon (fortunately for people who live on planets in dwarf galaxies!) that can produce some spectacular results. One of the best examples of this occurring is in the relatively

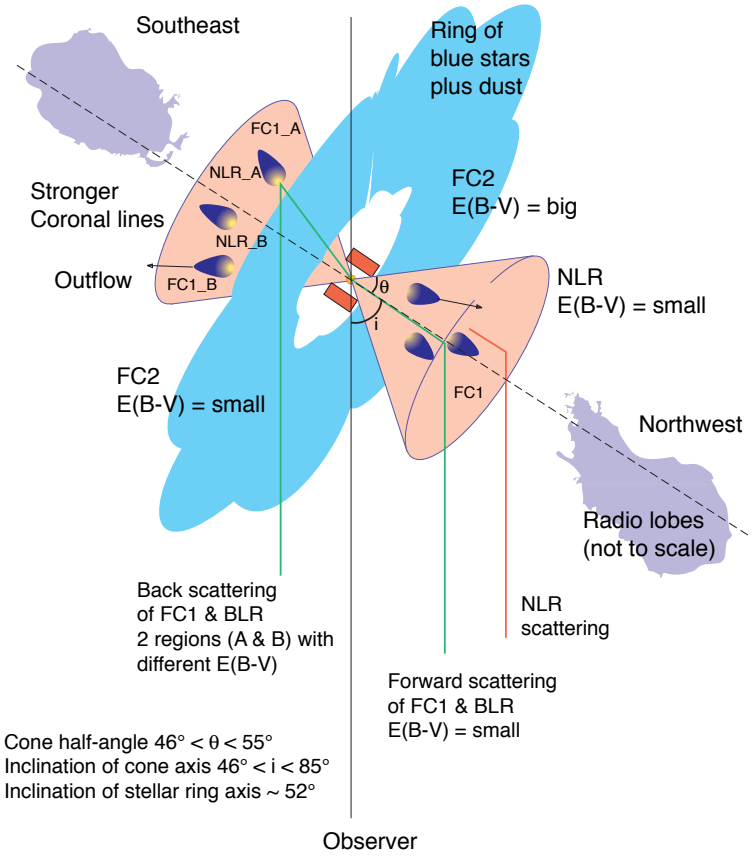

Fig. 9. A cartoon of *Cygnus A* which illustrates the various components, their positions and orientations. The letters 'FC' followd by a number represent various so-called 'featureless continua' that had been seen in the spectropolarimetry as polarized or unpolarized sources.

nearby radio galaxy PKS B2152-699 ($z = 0.0282$). Fig.10 shows an optical (HST) and radio (ATCA) image of the galaxy with a 'shredded' gaseous cloud (HIC) some 8kpc out along the radio axis: actually along the extension of the axis defined by the VLBI jet on a scale of a few tens of mas [4]. Optical spectroscopy has shown this cloud to have a very highly excited emission line spectrum, including a strong [Fe X] coronal line. It also emits (or scatters) a very blue, polarized optical/near-UV continuum. In addition to a radio component slightly offset from the optical cloud, there is an associated X-ray source seen with both ROSAT and Chandra. Detailed, multiwavelength stud-

ies of sources such as this give us an excellent opportunity to measure the properties and makeup of the particle jet and its associated photon beam.

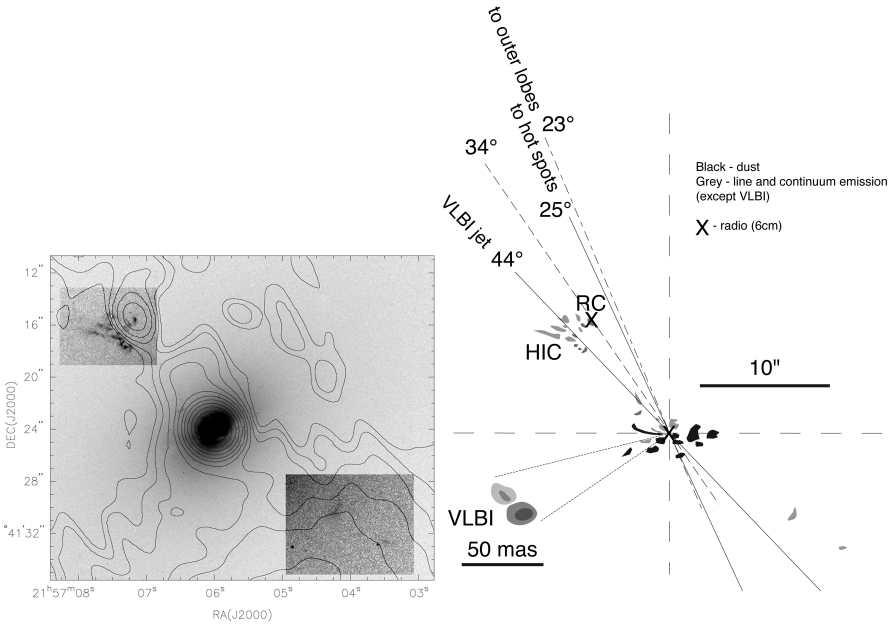

Fig. 10. An optical image (greyscale, HST WFPC 2) and a radio map (contours, ATCA) of the radio galaxy PKS B2152-699 showing the bright jet-cloud interaction (HIC) to the NE and a fainter counter feature to the SW. The associated cartoon illustrates the location and the orientation of the various observed components with 'RC' marking the offset position of the 6cm radio source associated with the HIC.

3.2 Distant AGN

The space density of powerful AGN was highest during the so-called 'Quasar Epoch' at redshifts around 2–3, corresponding to lookback times of around 10 billion years. This was the time when the most massive galaxies were forming in environments that were to become the rich clusters we see today. The presence of luminous active nuclei in these galaxies has a significant effect on their surroundings and, fortunately for us, 'illuminates' structures and processes that we should otherwise find it very difficult to study. The ionization cones represent the ISM of the host galaxy ionized by the hard AGN spectrum and, with a suitable understanding of the photoionization physics, allows the study of the chemical composition and the kinematic state of the gas. A *disadvantage* of the presence of the AGN is, however, the

extent to which its effects can dominate the other source of luminosity, i.e., the stellar population. Efforts to look at the stellar evolutionary properties of those galaxies that contain a currently active AGN are seriously hampered in the restframe ultraviolet and optical wavebands where the young populations should be most accessible. Studies of more evolved populations in the NIR are, in principle, less disturbed but do require the ability to observe at wavelengths inaccessible from the ground.

The most detailed studies of AGN host galaxies in the Quasar Epoch have been those of the powerful radio galaxies since these are our only currently complete samples of high redshift type 2 objects. Radio-quiet type 2 sources are beginning to be found now as a result of deep surveys in (hard-ish) X-ray bands and, most recently, in the mid-infrared. While we recognise that the radio-loud sources do not represent the entire AGN host population, we do believe that they mark the most massive galaxies in the Universe.

At a redshift of around 2.5, the restframe ultraviolet spectrum (from Lyman-α to C III] λ1909) and beyond is accessible to optical instruments while the NIR instruments nicely accommodate, within the J, H and K-bands, the important optical emission lines from [O II] λ3727 to Hα, [N II] and [S II] in the red. An example of such a source, observed in the optical with the Keck II instrument LRIS and in the NIR with ISAAC on the VLT, is shown in Fig. 11. While this object is extreme in the sense that it appears to be completely dominated by reflected light from the obscured quasar, it does caution us about the difficulty of accessing the underlying stellar population.

The detailed nature of the scattering process that we see at work in an object like this and producing a high redshift example of the alignment effect has been the subject of much discussion. The fact that the scattering appears to be almost perfectly grey, with the reflected continuum and broad emission lines being so well represented by a bright quasar reduced in intensity by around 3 magnitudes, suggests Thompson scattering as the responsible mechanism. It can be shown, however, that a dusty medium consisting of optically thick clumps embedded in a thin intraclump medium, makes an efficient grey scatterer without broadening spectral features to the extent that would occur after scattering by hot electrons [18], [14], [15]. The physics of this process is rather simple and worth understanding because of its general applicability in complex geometries.

Assume that the AGN is surrounded by such a clumpy, dusty medium but completely obscured from our direct view. An emergent photon is scattered into our line of sight with a probability determined by the scattering optical depth along its original path. On its route to the observer, the photon suffers the possibility of being either scattered out of our line of sight or of being absorbed by a dust grain. The scattered source is consequently attenuated by an extinction optical depth, giving an emergent luminosity

$$L_{obs} \propto L_{AGN}(\lambda) \times \tau_{scat}(\lambda) \times e^{-\tau_{ext}(\lambda)}$$

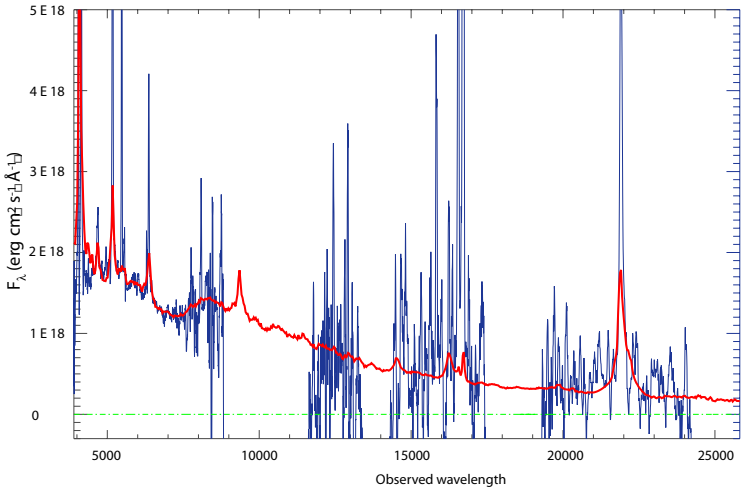

Fig. 11. The ultraviolet–optical SED of the radio galaxy TXS 0211-122, $z = 2.340$ measured with the Keck (optical) and VLT (NIR) telescopes. The red line shows a template radio-loud quasar spectrum scattered by a clumpy dust distribution within the illuminated 'ionization cones' in the host galaxy. In this powerful source, the entire UV-optical continuum can be ascribed to the scattered AGN light which completely dominates the host galaxy starlight. The narrow emission lines—which are relatively much stronger than in the scattered quasar light—originate from the photoionized ISM of the host. The shortest wavelength emission line is Lyman-α and the redmost line is Hα. (Courtesy J. Vernet et al.)

where $L_{AGN}(\lambda)$ is the quasar luminosity. This function is a maximum when $\tau_{scat}(\lambda) \simeq \tau_{ext} \simeq 1$. A geometrically complex scattering medium acts, therefore as a self-regulating 'mirror' that reflects a wavelength-independent fraction of the source, i.e., as a grey scatterer. Galactic dust has extinction and scattering cross sections that are proportional to one another throughout the UV-optical spectrum except close to the resonance at 2200Å. This has the result that, while the overall scattered spectrum is grey, a 2200Å feature is imprinted on the emergent spectrum. This can be seen as the bump around an observed wavelength of 8000Å in the observed and modelled spectra in Fig. 11.

Spectropolarimetry of the powerful $z \sim 2.5$ radio galaxies shows spatially-averaged fractional polarizations from zero ($\leq$ 2 or 3%) up to 25% in the continuum longward of Lyman-α (see Fig.12 for an example of a high polarization source). This suggests the presence of an unpolarized continuum source in some of the objects in addition to the dust-scattered quasar. It

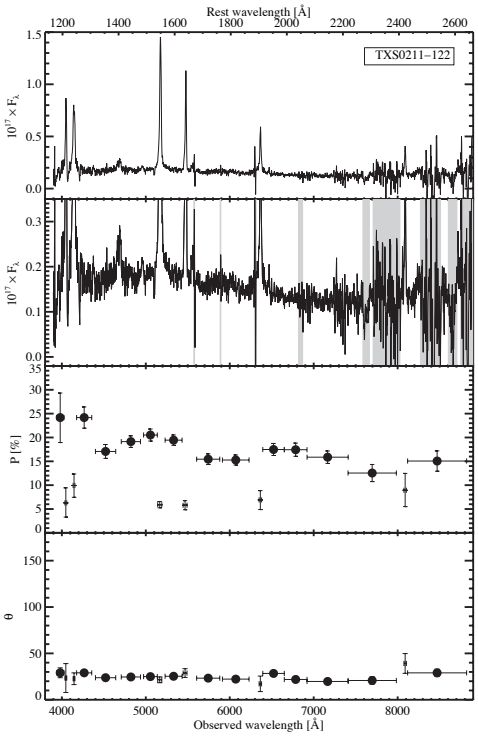

Fig. 12. Optical spectropolarimetry of TXS 0211-122 obtained with the Keck LRISp instrument. The top two panels show differently scaled versions of the total flux. The third panel shows the fractional polarization in both line and continuum wavelength bins. The final (bottom) panel shows the position angle of the ***E***-vector in the same wavelength bins: for comparison, the PA of the major axis of the restframe UV image of this source is 122° which is geometrically consistent with the scattering origin of the alignment effect. The degree of polarization is also consistent with dust (single-)scattering models within ionization cones where the integration over scattering angle dilutes the net polarization. Note the low fractional polarization in the narrow bands centred on the strong, narrow emission lines. (Courtesy J. Vernet et al.)

is natural to assume that this is starlight—although it is very difficult to demonstrate this conclusively by searching for UV absorption lines from hot star photospheres. Some photospheric lines have been reported but these are not always seen in the spectra of high redshift radio source hosts even with long exposures on the biggest telescopes [2].

Evidence for high rates of star formation in these massive galaxies probably comes more directly from observations of the heat radiated by the large scale dust distribution. Fig. 13 suggests that the bulk of FIR/sub-mm ther-

mal emission observed from these massive objects is unlikely to come from the AGN-heated dust within the ionization cones. It is more likely to come, instead, from dust-obscured star formation which must be occurring in these objects at this epoch. The hotter AGN-heated dust in the nuclear regions (torus) will radiate at much shorter wavelengths in the MIR.

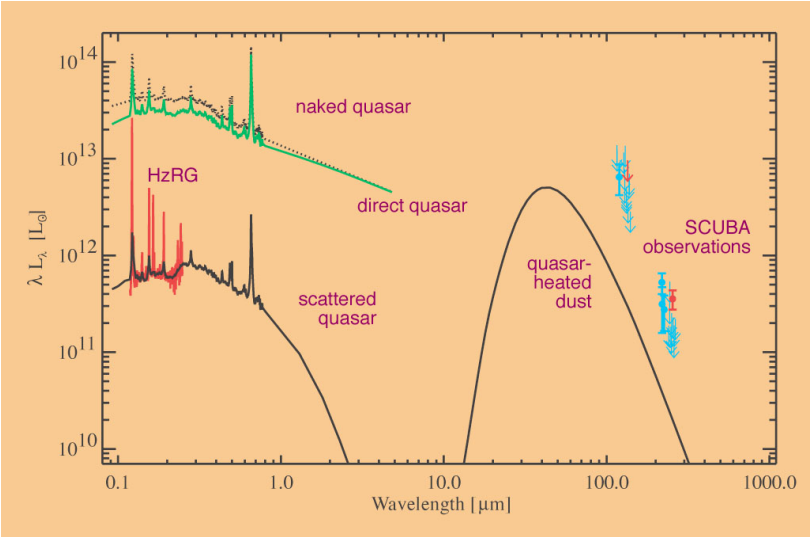

Fig. 13. A diagram representing the scattering, absorption and thermal emission balance for the dust content of the ionization cones (*only*) in an type 2 active galaxy. Starting with the naked quasar SED in the upper left corner, the lower green line represents the escaping flux after some modest dust extinction when seen close to the AGN axis (as a type 1 object). The lower left black line represents the quasar light scattered out of the ionization cone, by the same dust that produces the extinction for a type 1 observer, towards an observer who would see this as a type 2 object. The red spectrum is an observation of one of the redshift 2.5 radio galaxies. The FIR SED (black curve on the right) is the thermal emission from the dust that is causing the extinction and scattering within the cones. The red sub-mm points are observations of the source represented by the red spectrum and the blue observations represent other high-z radio galaxies. This analysis suggests that the bulk of the cool dust thermal emission from AGN like this is coming from dust heated by star formation rather than being reprocessed quasar power. (Courtesy J. Vernet et al.)

Another observational characteristic of these sources is the presence of huge gaseous halos seen in the Lyman-α line as emission that is sometimes overlayed with spatially extended narrow absorption. These halos can be seen on scales of 100kpc or more and have luminosities of 10^{43-44}erg s^{-1} [16], [11]. Fig. 14 shows long-slit spectra of TXS 0211-122 aligned with its HST image

and VLA radio map. Other UV lines are spatially extended but usually not to the extent of Lyman-α. Kinematically, these halos appear to divide into two zones, one that is highly disturbed and probably associated with the passage of the jet and another that is more quiescent and may represent the remnants of the gaseous reservoir from which the galaxy is forming.

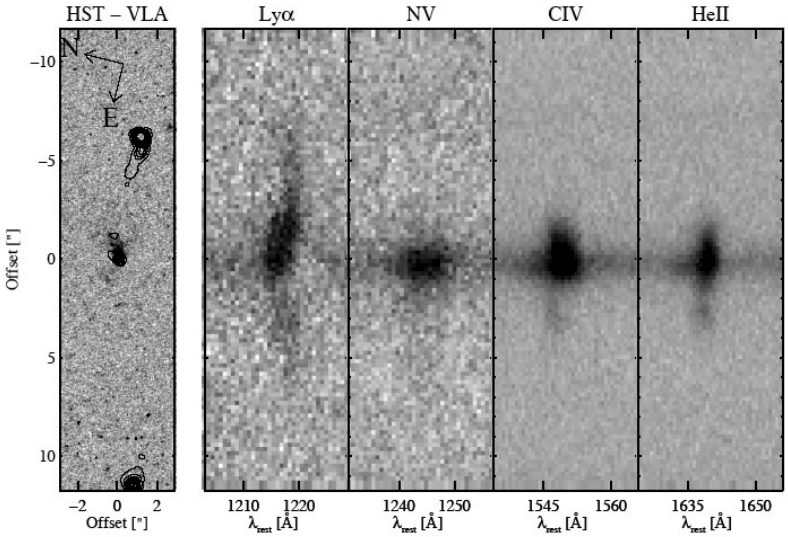

Fig. 14. The emission line halo of TXS 0211-122 from Keck long-slit spectroscopy. The halo can be seen in all the strong UV emission lines but is most extended in Lyman-α. the spectra are plotted aligned and on the same spatial scale as the restframe UV and radio images. Some of these halos can be detected even beyond the extent of the radio lobes. (Courtesy M. Villar-Martín et al.)

The line-emitting photoionized gas in the AGN host galaxies can provide a measure of the chemical composition of the ISM and so provide an important indicator of the galaxy's evolutionary history. Early studies of the EELR in low redshift, radio-loud AGN hosts showed that the extended gas generally has approximately Solar composition with remarkably little variation from object to object. Such apparent uniformity suggests that the current state of the extended ISM in these massive galaxies is the result of a steady integration of star formation and gas mixing taking place over a long period of time. The ability, now provided by the large groundbased telescopes, to extend these studies to earlier epochs, offers the exciting opportunity to witness the build up of the metallicity during the assembly of the massive galaxies.

Since the optical spectrum gives us access to only the restframe UV of high redshift (within the 'quasar epoch') sources, it is necessary either to develop metallicity measures using these UV lines or to observe in the NIR

where the 'traditional' techniques developed for the optical spectrum can be employed. Both of these approaches are starting to be employed now but they still provide significant observational challenges. The UV spectrum is dominated by resonance lines of hydrogen, nitrogen, carbon and magnesium that are easy to measure but difficult to interpret since they are subject to optical depth effects and absorption by dust. There are reasonably prominent intercombination (semi-forbidden) lines of C,N, O and Si but these, while being easier to interpret, do require long integrations with the largest telescopes to measure with any precision. In the restframe optical band, we are on more familiar territory with the traditional favourite forbidden spectra of N, O, Ne and S referenced to the Balmer series of H and the He II line at 4686Å. These lines come, however, at the cost of the bright NIR sky and the atmospheric absorption between the J, H and K-bands.

Analyses are carried out with the aid of photoionization models and some knowledge of the shape of the ionizing SED from the AGN. The results are generally presented and interpreted by plotting the line-ratio diagnostic diagrams that have become familiar in the field. Models are run with sequences of ionization parameter U, gas metallicity and ionizing SED shape (e.g., power law slope) and compared with the observed points in different diagrams that have different dependencies on the input parameters. Ratios are chosen to be as independent as possible of the effects such as dust reddening. As usual, difficulties arise in the detail: the effects of dust on resonance line transfer means that gas clouds look very different when seen from their illuminated and shadowed sides. Also, gas clouds that are transparent to the ionizing continua ('matter bounded') and opaque ('ionization bounded') can produce different spectra for a given set of basic input parameters. However, there are clear trends apparent in the observational data that currently challenge our interpretational ability. An example is the C IV, N V, He II diagram that has been used for a decade or more to interpret the BLR of quasars. This is shown for the NLR of radio galaxies in Fig. 15. While diagrams such as these suggest a broader range in gas metallicity than seen within quasar hosts at the current epoch, there is still a need for confirmation using the forbidden line ratio diagrams that require NIR spectroscopy at the higher redshifts.

4 What next?

The deep surveys currently being carried out from the X-ray to the radio, including the important space-infrared capabilities, offer us the first opportunity for a rather complete census of both type 1 and type 2 AGN extending to the highest redshifts. These sources will act as 'markers' for elucidating the relationship between star and SMBH formation in galaxies and the nature of the feedback process responsible for the close observed relationship between them. The host galaxies serve as 'bolometers' that allow luminosity estimates

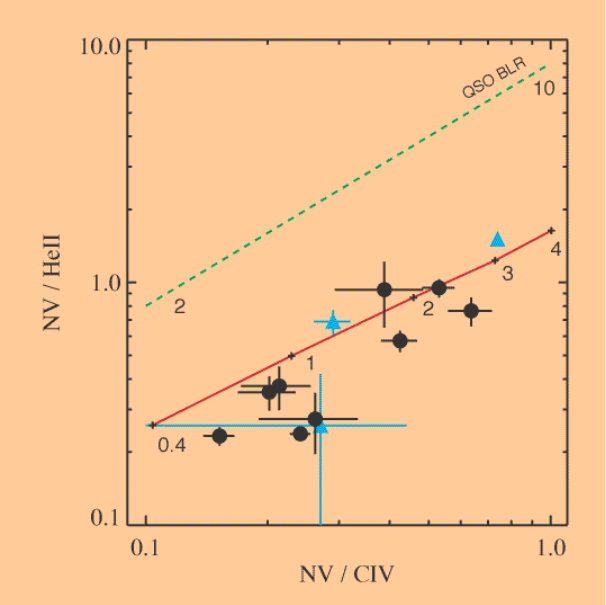

Fig. 15. An ultraviolet line ratio diagram plotted for the NLR radio galaxies at $2 \leq z \leq 3$. The red line shows a sequence of photoionization models as a function of metallicity in Solar units. The black and blue points are (similar) sources from different observed samples. The dashed green line shows the locus of points established for quasar BLR—which of course have a much higher particle density—again labelled with metallicity in Solar units. (Courtesy J. Vernet et al.)

even for the obscured type 2 sources, enabling us to complete the inventory of gravitational and nucleosynthetic photon production in the Universe.

Further detailed studies of individual objects will yield more information about the chemical evolution of massive galaxies at early epochs and, by discrimination between reprocessed AGN light and starlight, map their stellar evolutionary histories. While observations of AGN hosts at high redshift are observationally challenging, the AGN themselves are bright and their effects on the surrounding medium can be reasonably prominent and accessible to a broad range of observational techniques.

5 Further Reading

The ESO conference proceedings: "Extranuclear activity in galaxies", Garching, Germany, 1989; E.J.A. Meurs and R.A.E. Fosbury (eds.) will give a general introduction to the field.

Acknowledgments. While an article such as this, in not attempting to comprehensively review the field, represents a personal view, I should like to single out and thank several colleagues who have worked with me over the years in this area of astronomy. The work on radio galaxy polarimetry was started with Sperello di Serego Alighieri and Clive Tadhunter and was given a huge boost by Marshall Cohen who used significant amounts of his Keck observing time to help us study sources at $z \sim 2.5$. Luc Binette, Andy Robinson, Montse Villar-Martín and Joël Vernet have worked extensively on data acquisition, interpretation and modelling. Finally, I thank the organisers of the meeting in Santiago for giving me both the opportunity of presenting this work and also of assimilating the other overviews.

References

[1] Chambers, K. C., Miley, G. K., & van Breugel, W. 1987, Nature, 329, 604
[2] Chambers, K. C., Miley, G. K., & van Breugel, W. J. M. 1990, ApJ, 363, 21
[3] Ferrarese, L., & Merritt, D. 2000, ApJ, 539, L9
[4] Fosbury, R. A. E., Morganti, R., Wilson, W., Ekers, R. D., di Serego Alighieri, S., & Tadhunter, C. N. 1998, MNRAS, 296, 701
[5] Krolik, J. H. 1999, Active galactic nuclei : from the central black hole to the galactic environment /Julian H. Krolik. Princeton, N. J. : Princeton University Press, c1999.,
[6] McCarthy, P. J., van Breugel, W., Spinrad, H., & Djorgovski, S. 1987, ApJ, 321, L29
[7] McLure, R. J., & Dunlop, J. S. 2002, MNRAS, 331, 795
[8] Ogle, P. M., Cohen, M. H., Miller, J. S., Tran, H. D., Fosbury, R. A. E., & Goodrich, R. W. 1997, ApJ, 482, L37
[9] Osterbrock, D. E. 1989, Research supported by the University of California, John Simon Guggenheim Memorial Foundation, University of Minnesota, et al. Mill Valley, CA, University Science Books, 1989, 422 p.,
[10] Pelat, D., Alloin, D., & Fosbury, R. A. E. 1981, MNRAS, 195, 787
[11] Reuland, M., et al. 2003, ApJ, 592, 755
[12] Robinson, A., Binette, L., Fosbury, R. A. E., & Tadhunter, C. N. 1987, MNRAS, 227, 97
[13] Tadhunter, C., & Tsvetanov, Z. 1989, Nature, 341, 422
[14] Városi, F., & Dwek, E. 1999, ApJ, 523, 265
[15] Vernet, J., Fosbury, R. A. E., Villar-Martín, M., Cohen, M. H., Cimatti, A., di Serego Alighieri, S., & Goodrich, R. W. 2001, A&A, 370, 407
[16] Villar-Martín, M., Vernet, J., di Serego Alighieri, S., Fosbury, R., Humphrey, A., Pentericci, L., & Cohen, M. 2003, New Astronomy Review, 47, 291
[17] Wilson, A. S., Young, A. J., & Shopbell, P. L. 2000, ApJ, 544, L27
[18] Witt, A. N., & Gordon, K. D. 1996, ApJ, 463, 681
[19] Zurita Heras, J. A., Türler, M., & Courvoisier, T. J.-L. 2003, A&A, 411, 71